PHYSICAL REVIEW E **92**, 040801(R) (2015)

Exact coupling threshold for structural transition reveals diversified behaviors in interconnected networks

Faryad Darabi Sahneh,[1,*] Caterina Scoglio,[1] and Piet Van Mieghem[2]

[1] *Electrical and Computer Engineering Department, Kansas State University, Manhattan, Kansas 66506, USA*

[2] *Faculty of Electrical Engineering, Mathematics, and Computer Science, Delft University of Technology, Delft, The Netherlands*

(Received 20 August 2014; revised manuscript received 19 August 2015; published 5 October 2015)

An interconnected network features a structural transition between two regimes [F. Radicchi and A. Arenas, Nat. Phys. **9**, 717 (2013)]: one where the network components are structurally distinguishable and one where the interconnected network functions as a whole. Our exact solution for the coupling threshold uncovers network topologies with unexpected behaviors. Specifically, we show conditions that superdiffusion, introduced by Gómez *et al.* [Phys. Rev. Lett. **110**, 028701 (2013)], can occur despite the network components functioning distinctly. Moreover, we find that components of certain interconnected network topologies are indistinguishable despite very weak coupling between them.

DOI: 10.1103/PhysRevE.92.040801 PACS number(s): 89.75.Hc, 87.23.Cc, 89.20.−a

Several natural and human-made networks—such as power grids controlled by communications networks, contact networks of human and animal populations for transmission of zoonotic diseases, and transportation networks consisting of multiple modes (road, flights, railroads, etc.)—cannot be represented by simple graphs and have led [1] to the introduction of interdependent, interconnected, and multilayer networks in network science [2,3]. Interconnected networks are mathematical representations of systems where two or more simple networks, possibly with different functionalities, are coupled to each other. The omnipresence of interconnected networks has spurred a variety of research [4–7], with particular interest in dynamical processes such as percolation [8,9], epidemic spreading [10–13], and diffusion [14,15].

Recently, Radicchi and Arenas [16] and Gomez *et al.* [14] proposed a stylized interconnected network [17], consisting of two connected networks, G_A and G_B, each of size N, with one-to-one interconnection, as sketched in Fig. 1, where the interconnection strength between the layers is parametrized by a coupling weight $p > 0$.

Radicchi and Arenas [16] demonstrated the existence of a *structural transition* point p^*. Depending on the coupling weight p between the two networks, the collective interconnected network can function in two regimes: *if $p < p^*$, the two networks are structurally distinguishable; whereas if $p > p^*$, they behave as a whole*.

While studying diffusion processes on the same type of interconnected network in Fig. 1, Gomez *et al.* [14] observed *superdiffusion*: for sufficiently large p, the *diffusion in the interconnected network takes place faster than in either of the networks separately*. Superdiffusion arises due to the synergistic effect of the network interconnection and exemplifies a characteristic phenomenon in interconnected networks. Placement of the introduction point of superdiffusion with respect to the critical point p^* is missing in the literature.

Whereas the existence of a critical transition p^* was reported in [16], here, we determine the exact coupling threshold p^*. Our exact solution illuminates the role of each individual network component and their combined configuration on the structural transition phenomena and uncovers unexpected behaviors. Specifically, we show structural transition is not a necessary condition for achieving superdiffusion. Indeed, superdiffusion can be achieved for a coupling weight p even below the structural transition threshold p^*, which is surprising because, intuitively, synergy is not expected if the network components are functioning distinctly. Moreover, we observe that the structural transition disappears when one of the network components has vanishing algebraic connectivity [18–20], as is the case for a class of scale-free networks. Therefore, components of such interconnected network topologies become indistinguishable despite very weak coupling between them.

Spectral analysis plays a key role in understanding interconnected networks. Hernandez *et al.* [21] found the complete spectra of interconnected networks with identical components. Sole-Ribalta *et al.* [22] studied the interconnection of more than two networks with an arbitrary one-to-one correspondence structure. Sanchez-Garcia *et al.* [23] employed eigenvalue interlacing [18] to provide bounds for the Laplacian spectra of an interconnected network with a general interconnection pattern. In addition, in a similar context of structural transition as [16], D'Agostino [24] showed that adding interconnection links among networks causes structural transition. For a class of random network models, specified by an intralayer [25] and an interlayer degree distribution, Radicchi [26] showed when the correlation between intralayer and interlayer degrees is below a threshold value, the interconnected networks become indistinguishable.

We study the interconnected network $\boldsymbol{G}$ of Radicchi and Arenas [16], and Gomez *et al.* [14], as depicted in Fig. 1. Matrices A and B represent the adjacency matrices of G_A and G_B, respectively. The overall adjacency matrix and Laplacian matrix [18] of the interconnected network $\boldsymbol{G}$ are

$$\boldsymbol{A} = \begin{bmatrix} A & pI \\ pI & B \end{bmatrix} \quad \text{and} \quad \boldsymbol{L} = \begin{bmatrix} L_A + pI & -pI \\ -pI & L_B + pI \end{bmatrix},$$

where L_A and L_B are the Laplacian matrices of G_A and G_B, respectively, and I is the identity matrix. The eigenvalues of the Laplacian matrix $\boldsymbol{L}$, denoted by $0 = \lambda_1 < \lambda_2 \leqslant \cdots \leqslant \lambda_{2N}$,

*Corresponding author: faryad@ksu.edu

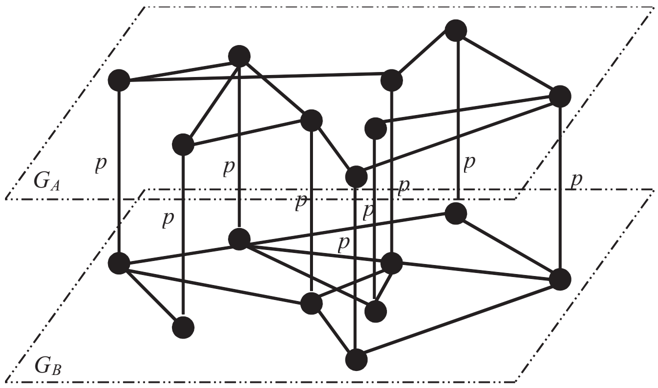

FIG. 1. One-to-one interconnection of two networks G_A and G_B, where the coupling weight is $p > 0$.

are the solutions of the eigenvalue problem

$$\begin{bmatrix} L_A + pI & -pI \\ -pI & L_B + pI \end{bmatrix} \begin{bmatrix} v_A \\ v_B \end{bmatrix} = \lambda \begin{bmatrix} v_A \\ v_B \end{bmatrix}, \tag{1}$$

where v_A and v_B contain elements of the eigenvector $\boldsymbol{v} = [v_A^T, v_B^T]^T$ corresponding to G_A and G_B, respectively, and satisfy the following eigenvector normalization:

$$v_A^T v_A + v_B^T v_B = 2N. \tag{2}$$

The *algebraic connectivity* $\lambda_2(\boldsymbol{L})$ of the interconnected network is the smallest positive eigenvalue of the Laplacian matrix $\boldsymbol{L}$ and the *Fiedler vector* $\boldsymbol{v}_2$ is its corresponding eigenvector. Algebraic connectivity of networks has been studied in depth [18,20] since Fiedler's seminal paper [19]. Algebraic connectivity quantifies the connectedness of a network and specifies the rate of convergence in a diffusion process [27] to its steady state. The Fiedler vector plays a key role in spectral partitioning of networks (see, e.g., [18]).

Superdiffusion occurs if the algebraic connectivity $\lambda_2(\boldsymbol{L})$ of the interconnected network is larger than the algebraic connectivity of each network component [14],

$$\lambda_2(\boldsymbol{L}) > \max\{\lambda_2(L_A), \lambda_2(L_B)\}. \tag{3}$$

Condition (3) indicates that diffusion in the interconnected network $\boldsymbol{G}$ spreads faster than in G_A or G_B if isolated. This condition does not hold for all interconnected networks. Gomez *et al.* [14] proved a necessary condition for superdiffusion is to have $\frac{1}{2}\lambda_2(L_A + L_B) > \max\{\lambda_2(L_A), \lambda_2(L_B)\}$. In this case, the criterion (3) for superdiffusion is met for sufficiently large coupling weights, since the algebraic connectivity $\lambda_2(\boldsymbol{L})$ is a monotone function of the coupling weight p and increases from 0 when $p = 0$, to $\frac{1}{2}\lambda_2(L_A + L_B)$ as $p \to \infty$.

The structural transition phenomenon of [16] can be understood through the behavior of the Fiedler vector of the interconnected network as a function of coupling weight p. For the eigenvalue problem (1), $\lambda = 2p$ and $v_A = -v_B = u \triangleq [1, \ldots, 1]^T$ is always a solution [14,16]. Therefore, if the coupling weight p is small enough, the algebraic connectivity of the interconnected network is $\lambda_2(\boldsymbol{L}) = \lambda = 2p$. Thus, the Fiedler vector $\boldsymbol{v}_2 = [u^T, -u^T]^T$ corresponding to $\lambda_2(\boldsymbol{L}) = 2p$ indicates that networks G_A and G_B are structurally distinct [16]. By increasing the coupling weight p, the eigenvalue $\lambda = 2p$ may no longer be the smallest positive one. Radicchi and Arenas [16] showed the existence of a structural transition at a threshold value p^* such that for $p > p^*$, the eigenvalue $\lambda = 2p$ exceeds the algebraic connectivity $\lambda_2(\boldsymbol{L})$, thus indicating an abrupt structural transition. Moreover, Radicchi and Arenas [16] argued that the coupling threshold is upper bounded by one fourth of the algebraic connectivity of the *superpositioned network*G_s with adjacency matrix $A + B$, which is equivalent to

$$p^* \leqslant \frac{1}{2}\lambda_2\left(\frac{L_A + L_B}{2}\right). \tag{4}$$

Although the coupling threshold p^* is a critical quantity for interconnected networks, little is known apart from the upper bound (4). We now explain our new method to find the exact expression for the coupling threshold p^*.

Since elements of the Laplacian matrix $\boldsymbol{L}$ are continuous functions of p, so are its eigenvalues [28]. This implies that the transition in the Fiedler vector of the interconnected network is not a result of any abrupt transition of the eigenvalues of $\boldsymbol{L}$, but rather due to crossing of eigenvalue trajectories as functions of p. Specifically, the Fiedler vector transition occurs precisely at the point where the second and third eigenvalues of $\boldsymbol{L}$ coincide. Therefore, *coupling threshold p^* is such that $\lambda = 2p^*$ is a positive, repeated eigenvalue of $\boldsymbol{L}$.*

As detailed in the Supplemental Material ([29], Sec. B.i.) we find that repeated eigenvalues occur at $\lambda = 2p^*$ for $N - 1$ different values of p^*, namely, $p^* = \frac{1}{2}\lambda_i(Q)$ for $i \in \{2, \ldots, N\}$, where Q can be expressed in the following forms ([29], Sec. B.ii):

$$Q \triangleq \bar{L} - \tilde{L}\bar{L}^{\dagger}\tilde{L} \tag{5}$$

$$= 2\left(L_A - \tfrac{1}{2}L_A\bar{L}^{\dagger}L_A\right) = 2\left(L_B - \tfrac{1}{2}L_B\bar{L}^{\dagger}L_B\right) \tag{6}$$

$$= L_A\bar{L}^{\dagger}L_B = L_B\bar{L}^{\dagger}L_A, \tag{7}$$

where $\bar{L} \triangleq \frac{1}{2}(L_A + L_B)$, $\tilde{L} \triangleq \frac{1}{2}(L_A - L_B)$, and the superscript † denotes the Moore-Penrose pseudoinverse [18]. Transition in the algebraic connectivity occurs at the coupling threshold corresponding to the smallest positive eigenvalue of Q, i.e.,

$$p^* = \tfrac{1}{2}\lambda_2(Q). \tag{8}$$

Furthermore, the coupling threshold p^* can be alternatively obtained as ([29], Sec. B.viii.)

$$p^* = \frac{1}{\rho(L_A^{\dagger} + L_B^{\dagger})}, \tag{9}$$

where $\rho(\bullet) \triangleq \lambda_N(\bullet)$ denotes the spectral radius [18].

The exact coupling threshold equation (8) depends, in a nonlinear way, on the matrices L_A, L_B, $\bar{L}$, and $\tilde{L}$ in Eqs. (5)–(3), and reveals that the structural transition phenomenon is jointly caused by A and B. Unfortunately, the exact solution (8) *implicitly* includes the joint influence of the network components.

However, the exact solution for the coupling threshold can lead to several lower and upper bounds for p^* with simple, physically informative expressions. Some of these bounds can be expressed only in terms of the algebraic connectivity of each isolated network G_A and G_B, as well as the superpositioned network G_s, as ([29], Secs. B.iv. and B.v.)

$$p^* \geqslant \frac{1}{\lambda_2^{-1}(L_A) + \lambda_2^{-1}(L_B)}, \tag{10}$$

$$p^* \leqslant \min\left\{\lambda_2(L_A), \lambda_2(L_B), \frac{1}{2}\lambda_2(\bar{L})\right\}. \tag{11}$$

We can furthermore find expressions that include *explicit* quantities pertaining to the network components jointly. We refer to such quantities as *interrelation* descriptors. As an example, we have obtained a class of upper bounds $p^* \leqslant \frac{1}{\bar{\rho}_{n_A, n_B}}$ that depend on the inner product of the eigenvectors of G_A and G_B with tunable accuracy and low computational cost as discussed in detail in [29], Sec. B.biii.. For further discussions on the network interrelation concept, readers can refer to [29], Sec. C.

Expression (10) elegantly lower bounds p^* by half of the harmonic mean of $\lambda_2(L_A)$ and $\lambda_2(L_B)$, and *is exact if* $v_{2A} = v_{2B}$. The upper bounds (11) not only include the upper bound (4), proposed in [16], but also exhibit a fundamental property of interconnected networks: *the coupling threshold* p^* *is upper bounded by the algebraic connectivity of each network component.*

Interestingly, if the algebraic connectivity of one network, say G_A, is much smaller than that of the other network G_B, then the network component with the smallest algebraic connectivity, here G_A, prominently determines the coupling threshold; but neither G_B nor the superpositioned network G_s play a major role. Indeed, if $K \triangleq \lambda_2(L_B)/\lambda_2(L_A) > 3$, then ([29], Sec. B.vi.)

$$\frac{K}{1+K}\lambda_2(L_A) < p^* \leqslant \lambda_2(L_A). \tag{12}$$

A corollary of Eq. (12) is if one of the network components has a vanishing algebraic connectivity, which is the case for a class of scale-free networks where $\lambda_2 \sim (\ln N)^{-2}$ [30], then $p^* \to 0$, indicating the transition point also disappears. Therefore, in such cases, even a very small coupling weight p leads to structural transition. This result is physically intuitive because a network with a small algebraic connectivity is vulnerable and loses its unity in response to external perturbations such as removal of a few edges or nodes or, as our analysis suggests, a weak coupling to another network.

Considering the opposite situation where the algebraic connectivity values of both networks are close to each other, we can show $p^* > \frac{1}{2}\max\{\lambda_2(L_A), \lambda_2(L_B)\}$ if the Fielder vectors are far from being parallel (see [29], Sec. B.vii.). As a consequence, for each coupling weight p satisfying $\frac{1}{2}\max\{\lambda_2(L_A), \lambda_2(L_B)\} < p \leqslant p^*$, we have

$$\lambda_2(\boldsymbol{L}) = 2p > \max\{\lambda_2(L_A), \lambda_2(L_B)\}. \tag{13}$$

Comparison of Eq. (13) with the superdiffusion criterion (3) reveals the counterintuitive finding that *superdiffusion, a synergistic characteristic phenomenon of an interconnected network, can occur for values of* $p < p^*$*, where the network components function distinctly!*

As mentioned above, the condition that Fielder vectors of G_A and G_B are far from being parallel is necessary for superdiffusion before structural transition. We find that this condition is indeed general to superdiffusion, regardless of structural transition; because close-to-parallel Fielder vectors of G_A and G_B yield $\lambda_2(\frac{L_A+L_B}{2}) \simeq \frac{\lambda_2(L_A)+\lambda_2(L_B)}{2}$, the necessary condition for superdiffusion, i.e., $\lambda_2(\frac{L_A+L_B}{2}) > \max\{\lambda_2(L_A), \lambda_2(L_B)\}$ can never be satisfied even for $p \to \infty$. This condition has a very interesting physical interpretation. When $p \to \infty$, corresponding nodes in G_A and G_B become a single entity. According to the important role of the Fiedler vector in graph partitioning, having close-to-orthogonal Fiedler vectors of G_A and G_B means that links of G_B connect those nodes that are far from each other in G_A, and vice versa. Therefore, with close-to-orthogonal Fiedler vectors of G_A and G_B, the overall interconnected network gains increased connectivity among its nodes compared to each isolated component, thus making superdiffusion feasible.

It is important to distinguish between speed of diffusion, determined by the smallest positive eigenvalues of the Laplacian matrix, and the mode of diffusion, determined by the corresponding eigenvectors. Superdiffusion concerns the speed of diffusion, while structural transition corresponds to an abrupt change in modes of diffusion. It would be a wrong idea to assume $p < p^*$ indicate that G_A and G_B are independents (expect for the trivial case of $p = 0$). The key point is that having $p < p^*$ simply implies that G_A and G_B are distinguishable. Before the structural transition the network components do interact with each other, and as we showed, can even positively favor the diffusion process speed as the result of increased overall connectivity in the interconnected network.

To illustrate our analytical assertions, we perform several numerical simulations. We generate an interconnected network with $N = 1000$, where the graph G_A is a scale-free network

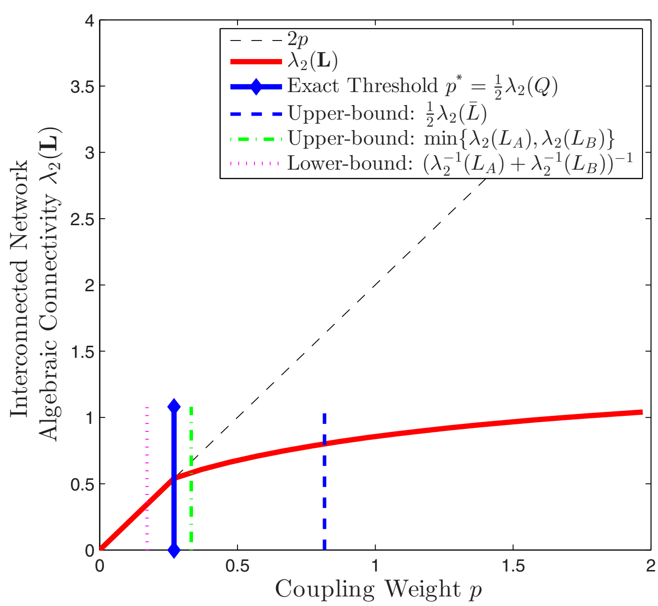

FIG. 2. (Color online) Algebraic connectivity $\lambda_2(\boldsymbol{L})$ of an interconnected network with scale-free G_A and random geometric G_B as a function of the coupling weight p. For $p < p^* \simeq 0.27$, algebraic connectivity is $\lambda_2(\boldsymbol{L}) = 2p$. For $p > p^*$, eigenvalue $\lambda = 2p$ is no longer the algebraic connectivity of the interconnected network; thus, denoting a structural transition at $p = p^*$.

according to the configuration model [31] with exponent $\gamma = 3$, and G_B is a random geometric network [32] with threshold distance $r_c = \sqrt{\frac{5 \ln N}{\pi N}}$. For generating the random geometric network, N nodes are uniformly and independently distributed in $[0,1]^2$ at random, and nodes of at most distance r_c are connected to each other. For these networks, $\lambda_2(L_A) \simeq 0.355$ and $\lambda_2(L_B) \simeq 0.332$. Figure 2 shows the algebraic connectivity $\lambda_2(L)$ of the interconnected network as a function of the coupling weight p, and illustrates that Eq. (8) predicts the coupling threshold exactly. Furthermore, this simulation supports the analytic results for bounds in Eqs. (11) and (10).

To investigate structural implications of interconnected networks, we design numerical experiments emphasizing the role of network interrelation. We generate a set of interconnected networks with identical superpositioned networks. Therefore, differences in the outcomes do not depend on the superpositioned network. We generate $A = [a_{ij}]$ and $B = [b_{ij}]$ according to the following rule: $a_{ij} = a_{ji} = p_{ij} w_{ij}$ and $b_{ij} = b_{ji} = (1 - p_{ij}) w_{ij}$, where w_{ij} is an element of the weighted Karate Club adjacency matrix (see Fig. 3 in Ref. [33]), and p_{ij} is identically independently distributed on $[0,1]$ for $j < i$. Figure 3 shows different bounds for the coupling threshold versus the exact values. The upper bound $\frac{1}{2}\lambda_2(\bar{L})$ remains constant, even though the exact threshold p^* has a broad distribution. When p^* is small, the upper bound $\frac{1}{2}\lambda_2(\bar{L})$ is loose, while the upper bound $\min\{\lambda_2(A), \lambda_2(B)\}$ is tight, as supported by Eq. (12). If one network component possesses a relatively small algebraic connectivity, Eq. (12) predicts that the coupling threshold p^* is determined by the algebraic connectivity of that component.

In conclusion, we derive the exact critical value p^* for the coupling weight in the interconnected network of Fig. 1. In addition to the graph properties of each network component individually, we find that the inner product of Fielder vectors of network components is an important interrelation descriptor for the structural transition phenomenon (see [29], Sec. A.iv., Fig. 4, for supporting numerical experiments). Other interrelation descriptors, such as the commonly used degree correlation [34–37], do not necessarily yield similar results ([29], A.iv., Fig. 5). Even though the analysis has been performed for interconnection of two networks, we demonstrate in [29] (Sec. D) that our method can be readily generalized to multiple interconnected networks.

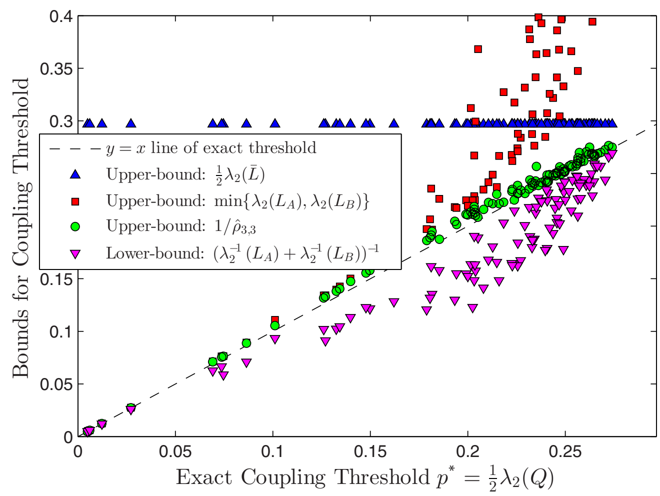

FIG. 3. (Color online) Bounds for the coupling threshold vs the exact values for a set of interconnected networks with identical averaged network. For each generated network, we compute different bounds for the coupling threshold and compare them with the exact value. The closer to the black dashed line $y = x$, the more accurate the bounds.

Our exact solution reveals diversified behaviors in interconnected networks, encompassing the case where the slightest coupling between network components results in a structural transition, as well as the case where coupling strength that is sufficiently large to cause superdiffusion is not large enough to cause structural transition. This emphasizes the importance and power of deliberate design for interconnected networks. In particular, our finding of superdiffusion without structural transition encourages further exploration of dynamical processes and interconnection architectures which allow the benefits of interconnections while preserving the autonomy of each subsystem.

The authors thank Filippo Radicchi, Alex Arenas, Aram Vajdi, Joshua Melander, and anonymous reviewers for their helpful suggestions to improve this manuscript. This work was supported by the National Science Foundation Award CIF-1423411.

[1] Such extensions have been presented in classical sociology literature such as H. C. White, S. A. Boorman, and R. L. Breiger, Am. J. Sociol. **81**, 730 (1976); which even dates back to L. von Wiese, *Sociology* (Oskar Piest, New York, 1941).

[2] M. Kivelä, A. Arenas, M. Barthelemy, J. P. Gleeson, Y. Moreno, and M. A. Porter, J. Complex Networks **2**, 203 (2013).

[3] S. Boccaletti, G. Bianconi, R. Criado, C. Del Genio, J. Gómez-Gardeñes, M. Romance, I. Sendiña-Nadal, Z. Wang, and M. Zanin, Phys. Rep. **544**, 1 (2014).

[4] J. Gao, S. V. Buldyrev, S. Havlin, and H. E. Stanley, Phys. Rev. Lett. **107**, 195701 (2011).

[5] J. Gao, S. V. Buldyrev, S. Havlin, and H. E. Stanley, Phys. Rev. E **85**, 066134 (2012).

[6] E. Estrada and J. Gómez-Gardeñes, Phys. Rev. E **89**, 042819 (2014).

[7] M. De Domenico, A. Solé-Ribalta, S. Gómez, and A. Arenas, Proc. Natl. Acad. Sci. USA **111**, 8351 (2014).

[8] S. V. Buldyrev, R. Parshani, G. Paul, H. E. Stanley, and S. Havlin, Nature **464**, 1025 (2010).

[9] Y. Hu, B. Ksherim, R. Cohen, and S. Havlin, Phys. Rev. E **84**, 066116 (2011).

[10] A. Saumell-Mendiola, M. Á. Serrano, and M. Boguñá, Phys. Rev. E **86**, 026106 (2012).

[11] M. Dickison, S. Havlin, and H. E. Stanley, Phys. Rev. E **85**, 066109 (2012).

[12] H. Wang, Q. Li, G. D'Agostino, S. Havlin, H. E. Stanley, and P. Van Mieghem, Phys. Rev. E **88**, 022801 (2013).

[13] F. D. Sahneh, C. Scoglio, and F. N. Chowdhury, in *American Control Conference (ACC), Washington, DC* (IEEE, Piscataway, NJ, 2013), pp. 2307–2312.

[14] S. Gómez, A. Diaz-Guilera, J. Gómez-Gardeñes, C. J. Pérez-Vicente, Y. Moreno, and A. Arenas, Phys. Rev. Lett. **110**, 028701 (2013).

[15] J. Aguirre, R. Sevilla-Escoboza, R. Gutiérrez, D. Papo, and J. M. Buldu, Phys. Rev. Lett. **112**, 248701 (2014).

[16] F. Radicchi and A. Arenas, Nat. Phys. **9**, 717 (2013).

[17] Such a topology is sometimes called a multiplex or more generally a multilayer network [2].

[18] P. Van Mieghem, *Graph Spectra for Complex Networks* (Cambridge University, Cambridge, England, 2011).

[19] M. Fiedler, Czech. Math. J. **23**, 298 (1973).

[20] N. M. M. de Abreu, Lin. Algebra App. **423**, 53 (2007).

[21] J. Martín-Hernández, H. Wang, P. Van Mieghem, and G. D'Agostino, Physica A **404**, 92 (2014).

[22] A. Solé-Ribalta, M. De Domenico, N. E. Kouvaris, A. Díaz-Guilera, S. Gómez, and A. Arenas, Phys. Rev. E **88**, 032807 (2013).

[23] R. J. Sánchez-García, E. Cozzo, and Y. Moreno, Phys. Rev. E **89**, 052815 (2014).

[24] G. D'Agostino, in *Nonlinear Phenomena in Complex Systems: From Nano to Macro Scale* (Springer, Berlin, 2014), p. 111.

[25] Intralayer links denote those within a single network, while interlayer links are those that connect two different networks.

[26] F. Radicchi, Phys. Rev. X **4**, 021014 (2014).

[27] The dynamic equation for a diffusion process on a graph with Laplacian matrix L follows $\dot{x} = -Lx$, which is the discretized equivalent of the heat equation $\partial_t \phi = \nabla^2 \phi$ for a continuous medium. Equation $\dot{x} = -Lx$ can also describe first-order consensus dynamics [see, e.g., R. Olfati-Saber, J. A. Fax, and R. M. Murray, Proc. IEEE **95**, 215 (2007)], analogous to a linearized synchronization equation [see, e.g., A. Arenas, A. Díaz-Guilera, J. Kurths, Y. Moreno, and C. Zhou, Phys. Rep. **469**, 93 (2008)].

[28] M. Zedek, Proc. Am. Math. Soc. Proc. **16**, 78 (1965).

[29] See Supplemental Material at http://link.aps.org/supplemental/10.1103/PhysRevE.92.040801 for mathematical proofs, additional numerical simulations, and extensions to more than two interconnected networks.

[30] A. N. Samukhin, S. N. Dorogovtsev, and J. F. F. Mendes, Phys. Rev. E **77**, 036115 (2008).

[31] B. Bollobás, Euro. J. Combinator. **1**, 311 (1980).

[32] M. Penrose, *Random Geometric Graphs*, Vol. 5 (Oxford University, Oxford, 2003).

[33] W. W. Zachary, J. Anthropol. Res. **33**, 452 (1977).

[34] J. Y. Kim and K.-I. Goh, Phys. Rev. Lett. **111**, 058702 (2013).

[35] B. Min, S. D. Yi, K.-M. Lee, and K.-I. Goh, Phys. Rev. E **89**, 042811 (2014).

[36] V. Nicosia and V. Latora, Phys. Rev. E **92**, 032805 (2015).

[37] V. Gemmetto and D. Garlaschelli, Sci. Rep. **5**, 9120 (2015).